Inorg. Chem. **2007**, *46*, 10510–10519

Theoretical Studies on Structures of Neptunyl Carbonates: $NpO_2(CO_3)_m(H_2O)_n^{q-}$ ($m = 1–3$, $n = 0–3$) in Aqueous Solution

K. Balasubramanian*,†,‡,§ and Zhiji Cao†

Department of Mathematics and Computer Science, California State University, East Bay, Hayward, California 94542, University of California, Chemistry and Material Science Directorate, Lawrence Livermore National Laboratory, Livermore, California 94550, and Glenn T. Seaborg Center, Lawrence Berkeley Laboratory, University of California, Berkeley, California 94720

Received March 13, 2007

Extensive ab inito computations have been carried out to study the equilibrium structure, infrared spectra, and bonding characteristics of a variety of hydrated $NpO_2(CO_3)_m^{q-}$ complexes by considering the solvent as a polarizable dielectric continuum as well as the corresponding anhydrate complexes in the gas phase. The computed structural parameters and vibrational results at the MP2 level in aqueous solution are in good agreement with Clark et al.'s experiments and provide realistic pictures of the neptunyl complexes in an aqueous environment. Our computed hydration energies reveal that the complex with water molecules directly bound to it yields the best results. Our analysis of the nature of the bonding of neptunyl complexes provides insight into the nature of 6d and 5f bonding in actinide complexes.

1. Introduction

Actinide migration in geological and biological environments has been a topic of prime concern in recent years.[1−16] Significant amounts of high-level nuclear wastes that are generated by a variety of nuclear activities are typically stored in deep geological repositories. The actinyl ions from these high-level wastes seem to migrate by solubility in groundwater or through other mechanisms such as sorption onto mobile colloidal silica. On the other hand, sorption onto geological minerals could prevent migration and thus there is considerable interest in the study of actinyl complexes with species in the groundwater under aqueous environmental conditions. Among nuclear waste products, neptunium has received particular attention due to its high solubility in groundwater and relatively low sorption with geological minerals that enhances its mobility. Consequently, neptunium complexes have been the topic of several experimental and theoretical studies.[1−18] Since CO_2 gas is ubiquitous in the environment, dissolved CO_2 in the groundwater could provide copious amounts of carbonic acid, which easily forms carbonate complexes for neptunyl ion speciation. In particular, neptunyl carbonate complexes play an important role in the process of radioactive transport, as these complexes with

* To whom correspondence should be addressed. E-mail: balu@csueastbay.edu. Fax: 925-422-6810.
† California State University, East Bay.
‡ Lawrence Livermore National Laboratory.
§ Lawrence Berkeley Laboratory.

(1) Maya, L. *Inorg. Chem.* **1984**, *23*, 3926.
(2) Grenthe, I.; Riglet, C.; Vitorge, P. *Inorg. Chem.* **1986**, *25*, 1679.
(3) Nash, K. L.; Cleveland, J. M.; Rees, T. F. *J. Environ. Radioact.* **1988**, *7*, 131.
(4) Nitsche, H.; Lee, S. C.; Gatti, R. C. *J. Radioanal. Nucl. Chem.* **1988**, *124*, 171.
(5) Nitsche, H.; Standifer, E. M.; Silva, R. J. *Lanthanide Actinide Res.* **1990**, *3*, 203.
(6) Nitsche, H. *Radiochim. Acta* **1991**, 52−3, 3.
(7) Palmer, P. D.; Clark, D. L.; Newton, T. W. *Abstr. Pap.—Am. Chem. Soc.* **1993**, *206*, 3.
(8) Pratopo, M. I.; Moriyama, H.; Higashi, K. *J. Nucl. Sci. Technol.* **1993**, *30*, 1024.
(9) Clark, D. L.; Hobart, D. E.; Neu, M. P. *Chem. Rev.* **1995**, *95*, 25.
(10) Moriyama, H.; Pratopo, M. I.; Higashi, K. *Radiochim. Acta* **1995**, *69*, 49.
(11) Palmer, P. D.; Clark, D. L.; Neu, M. P.; Tait, C. D.; Ekberg, S. A.; Newton, T. W. *Abstr. Pap.—Am. Chem. Soc.* **1995**, *209*, 6.
(12) Clark, D. L.; Conradson, S. D.; Ekberg, S. A.; Hess, N. J.; Janecky, D. R.; Neu, M. P.; Palmer, P. D.; Tait, C. D. *New J. Chem.* **1996**, *20*, 211.
(13) Clark, D. L.; Conradson, S. D.; Ekberg, S. A.; Hess, N. J.; Neu, M. P.; Palmer, P. D.; Runde, W.; Tait, C. D. *J. Am. Chem. Soc.* **1996**, *118*, 2089.
(14) Runde, W.; Neu, M. P.; Clark, D. L. *Geochim. Cosmochim. Acta* **1996**, *60*, 2065.
(15) Clark, D. L.; Conradson, S. D.; Neu, M. P.; Palmer, P. D.; Runde, W.; Tait, C. D. *J. Am. Chem. Soc.* **1997**, *119*, 5259.
(16) Kato, Y.; Kimura, T.; Yoshida, Z.; Nitani, N. *Radiochim. Acta* **1998**, *82*, 63.
(17) Gagliardi, L.; Roos, B. O. *Inorg. Chem.* **2002**, *41*, 1315.
(18) Vallet, V.; Macak, P.; Wahlgren, U.; Grenthe, I. *Theor. Chem. Acc.* **2006**, *115*, 145.

10.1021/ic700486u CCC: $37.00
Published on Web 11/14/2007

actinide ions are quite soluble in water.[3,4] Furthermore, investigations of the structures, spectra, and bonding of neptunyl carbonate complexes are of fundamental importance, as these complexes are central to our understanding of the coordination chemistry of actinide species, especially in the aqueous environment.

It is well-known that the neptunyl ion occurs as the Np(V) oxide ion in the environment or NpO_2^+, and thus, the carbonate complexes of Np(V) have been known for decades.[9,18] There are ample spectrophotometric and solubility data supporting the formation of monomeric complex anions, $NpO_2(CO_3)^-$, $NpO_2(CO_3)_2^{3-}$, and $NpO_2(CO_3)_3^{5-}$ in solution. In a series of pioneering studies, Clark and co-workers[12,13] have reported the first elucidation of the molecular structures of Np(V) carbonates in an aqueous solution through extended X-ray absorption fine structure spectroscopy (EXAFS), although earlier near-IR spectral studies by Nitsche and co-workers[5,6] as well as others have provided ample evidence that these complexes are present in multiple forms in aqueous solutions. These IR studies by Nitsche and co-workers[5,6] have revealed that solution complexes of Np(V) carbonates are in equilibrium with the solid phases and that the near-IR spectra of $NpO_2(CO_3)^-$, $NpO_2(CO_3)_2^{3-}$, and $NpO_2(CO_3)_3^{5-}$ in different electrolyte solutions are quite similar, indicating that all these species coexist in aqueous solutions.

Clark et al.[12,13] have found that the use of large, bulky cations such as $CH_3CH_2CH_2CH_2N^+$ in place of the more commonly used Na^+ and K^+ ions in the preparation of solutions of $NpO_2(CO_3)^-$, $NpO_2(CO_3)_2^{3-}$, and $NpO_2(CO_3)_3^{5-}$ affords a large solubility increase and thus facilitates the study of solution species using a variety of spectroscopic techniques, which were formidably difficult earlier due to the low concentrations of the ions. They have adopted a variety of methods such as NMR and NIR, Raman, and EXAFS spectroscopies to study the pentavalent neptunium carbonate complexes. The EXAFS data[13] for $NpO_2(CO_3)_3^{5-}$ reveal unequivocally that the three carbonate ligands bond to the NpO_2^+ center in a bidentate fashion in the equatorial plane, although the experimental results seem ambivalent concerning the number of water molecules bound to $NpO_2(CO_3)^-$ and $NpO_2(CO_3)_2^{3-}$ in an aqueous environment. Gagliardi and Roos[17] have carried out a computational study at the CASSCF/CASPT2 levels of the naked and the hydrated neptunyl carbonate complexes by modeling the solvent effect through a reaction field Hamiltonian with a spherical cavity. Although they employ different effctive core potentials, they have found that in the gas phase the Np(V)−monocarbonate complex has a pentacoordinated structure with three water molecules in the first coordination shell whereas the dicarbonate complex exhibits a hexacoordinated structure with two water molecules in the first coordination shell.[17] Moreover, they have found that in the gas phase the D_{3h} structure is a real minimum for $NpO_2(CO_3)_3^{5-}$ and have employed counterions to mimic the solvent effects. Their study shows that only minor geometrical rearrangements occur in the one-electron reduction of $NpO_2(CO_3)_3^{4-}$ to $NpO_2(CO_3)_3^{5-}$, thus confirming the reversibility of this reduction. The work of Gagliardi and Roos[17] has provided a high-level benchmark for the gas-phase complex, which we use in our work to calibrate the accuracy of other methods. We have shown here that the second-order Møller-Plesset perturbation (MP2) method for complexes in aqueous solution using the polarizable continuum model (PCM) as opposed to a spherical cavity yields very good results and provides an efficient and reasonable method to model such complexes in aqueous solution. Moreover, we compute the vibrational spectra, vibrational frequencies, and all thermodynamic properties in solution including Gibbs energies for these complexes in aqueous solution for the first time. There have also been other theoretical studies[19−25] concerning actinide species, especially in the gas phase, by Pyykkö and co-workers,[19,23] Hay and co-workers,[20] Pitzer and co-workers,[21] as well as Bursten's group.[22,24]

In a recent paper,[25] we reported that bulk solvent effects are important for modeling actinide complexes in the aqueous environment, and the solvent influences the structures and spectra of the hydrated actinyls, especially in regards to the An−OH_2 bonds as well as subtle variations in the An−O equatorial and axial bonds. Consequently, structural reoptimization of the complex in a dielectric cavity seems inevitable if one needs to seek subtle structural variations in the solvent and to correlate with the observed spectra in the aqueous environment. Moreover, the aqueous thermodynamic properties such as the solvation Gibbs energies can be obtained computationally only through modeling these complexes in aqueous solution. In the present work, we have carried out extensive ab initio calculations in order to obtain the equilibrium structure, vibrational frequencies, and bonding characteristics of the hydrated $NpO_2(CO_3)_m^{q-}$ complexes in aqueous solution. The solvent effects were considered using a combined discrete−continuum model[18] in which the ionic solute and the closest ligands around the solute are treated in a fully quantum mechanical method while the rest of the bulk solvent is considered via a continuum model. As we show here, a hybrid quantum−continuum model within the MP2 level of theory provides a very good description of the equilibrium geometries and the observed spectra in an aqueous environment, provided the complex is hydrated to the fullest extent possible and the hydrated complex is treated quantum chemically. In particular, we have optimized $NpO_2(CO_3)_m(H_2O)_n^{q-}$ ($m = 1-3$, $n = 0-3$) in solution through a polarizable continuum model at the B3LYP and MP2 levels. We have also compared our optimized gas-phase geometries obtained through these methods and the coupled cluster singles + doubles (CCSD) method with those from the CASSCF/CASPT2 methods[17]

(19) Pyykkö, P.; Li, J.; Runeberg, N. *J. Phys. Chem.* **1994**, *98*, 4809.
(20) Schreckenbach, G.; Hay, P. J.; Martin, R. L. *J. Comput. Chem.* **1999**, *20*, 70.
(21) Zhang, Z. Y.; Pitzer, R. M. *J. Phys. Chem. A* **1999**, *103*, 6880.
(22) Andrews, L.; Zhou, M. F.; Liang, B. Y.; Li, J.; Bursten, B. E. *J. Am. Chem. Soc.* **2000**, *122*, 11440.
(23) Straka, M.; Dyall, K. G.; Pyykkö, P. *Theor. Chem. Acc.* **2001**, *106*, 393.
(24) Li, J.; Bursten, B. E.; Liang, B. Y.; Andrews, L. *Science* **2002**, *295*, 2242.
(25) Cao, Z. J.; Balasubramanian, K. *J. Chem. Phys.* **2005**, *123*, 114309.

and have shown that the MP2 method is quite satisfactory, as the complexes are predominantly single configuration in nature.

2. Methods of Computation

All the calculations were carried out using relativistic effective core potentials (RECPs) which replace the 78 core electrons of neptunium.[26] We have also carried out comparison computations with small-core 60-core electron RECPs for Np. The 6s and 6p outer-core electrons, as well as the valence 5f, 6d, and 7s electrons, are explicitly treated using Gaussian basis sets, i.e., [5s3p3d2f] for Np.[26] An uncontracted [5s5p4d4f] basis set for Np was used in the calculations of energy separations. For the purpose of comparison, the Stuttgart basis set[27] combined with the 60-electron RECP[28] and Christiansen's unpublished basis set combined with the 68-electron RECP were also applied for $NpO_2(CO_3)_2^{3-}$. For the carbon and oxygen atoms, RECPs were employed retaining the outer 2s and 2p shells in the valence space, again choosing compatible valence Gaussian basis sets.[29] The carbon and oxygen basis sets from Pacios and Christiansen[29] were augmented with sets of six-component 3d Gaussian functions ($\alpha_d = 0.75$ for carbon and 0.85 for oxygen) adopted from Dunning and Hay.[30] The van Duijneveldt's hydrogen basis set[31] was used for the hydrogen atoms augmented by a set of polarization functions. Similar basis sets have been previously tested and utilized for uranyl complexes successfully.[25,32−34] In previous work, we tested the effects of 5g functions on the actinide and found these effects to be negligible and thus did not incorporate them in the present work to save computer time for intensive solvent and CCSD computations.

Equilibrium geometries in aqueous solution were optimized using the DFT[35] and MP2[36] approaches. In the gas phase, we have optimized the equilibrium geometries at all these levels and by the use of the CCSD method for the dicarbonate and monocarbonate of neptunyl ion. We have uniformly obtained the vibrational frequencies and IR spectra at all these levels to ensure that the computed optimized geometries are true minima and also to provide for the spectra of these species. The DFT approach utilized the B3LYP functional.[37−39] The effect of solvent (water) was studied using the self-consistent reaction field models, considering the solvent to be a dielectric continuum. The integral equation formalism PCM model (IEFPCM)[40−43] was used for this purpose. The geometries were fully optimized without symmetry restrictions using these models to seek their structures in aqueous solution. In the IEFPCM model, which has been previously utilized successfully,[25] the solute is immersed in a shape-adapted cavity defined by interlocking spheres centered on each solute atom or group and with standard UATM (united atomic topological model) radii.[43]

Scheme 1. Thermodynamic Cycle Considered for Calculating Solvation Gibbs Energies of the Solutes in Water

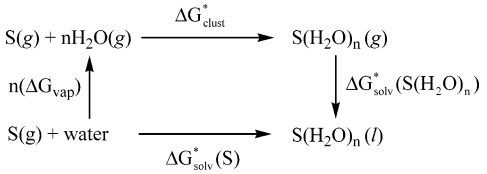

We have also carried out Gibbs energy computations in solution, which required the frequency calculations to characterize the stationary points in solution and to estimate the zero-point vibrational and entropy contributions to the Gibbs energies by using standard mechanical formulas[44] in the aqueous solution phases. The corresponding gas-phase complexes were also optimized to study the effect of solvation on geometries and spectra.

The discrete−continuum model has been applied to the calculations of the solvation Gibbs energies of ionic solutes from the thermodynamic cycle presented in Scheme 1. Thus, the solvation Gibbs energies are calculated as (S denotes the solute)

$$\Delta G^*_{solv}(S) = n\Delta G_{vap} + \Delta G^*_{clust} + \Delta G^*_{solv}(S(H_2O)_n)$$

where $n\Delta G_{vap}$ is the Gibbs energy required to move n water molecules from the pure liquid phase to the gas phase to form the cluster with the solute, ΔG^*_{clust} is the Gibbs energy of formation of the cluster $S(H_2O)_n$ in the standard state (1 mol/L), and $\Delta G^*_{solv}(S(H_2O)_n)$ is the solvation Gibbs energy of the cluster corresponding to the long-range interactions of the hydrated cluster embedded in a cavity, which refers to the process of gas (1 mol/L) → solution (1 mol/L).[45] For the Gibbs energy of vaporization of water, we have used the experimental value of 2.05 kcal/mol forΔG_{vap}.[46] It should be noted that the vaporization occurs under the pressure of 1 atm, and thus, an expansion work term $P\Delta V$ has been added to the Gibbs energy. All of the calculations were carried out using the *Gaussian 03* package of codes.[47]

3. Results and Discussion

We have carried out a series of computations of the structures and the IR spectra of complexes both in the gas

(26) Ermler, W. C.; Ross, R. B.; Christiansen, P. A. *Int. J. Quantum Chem.* **1991**, *40*, 829.
(27) Cao, X. Y.; Dolg, M.; Stoll, H. *J. Chem. Phys.* **2003**, *118*, 487.
(28) Kuchle, W.; Dolg, M.; Stoll, H.; Preuss, H. *J. Chem. Phys.* **1994**, *100*, 7535.
(29) Pacios, L. F.; Christiansen, P. A. *J. Chem. Phys.* **1985**, *82*, 2664.
(30) Dunning, T. H.; Hay, P. J. *Methods of Electronic Structure Theory*; Plenum: New York, 1977; p 1.
(31) van Duijneveldt, F. B. *IBM Tech. Res. Rep.* **1971**, *RF*945.
(32) Majumdar, D.; Roszak, S.; Balasubramanian, K.; Nitsche, H. *Chem. Phys. Lett.* **2003**, *372*, 232.
(33) Wheaton, V.; Majumdar, D.; Balasubramanian, K.; Chauffe, L.; Allen, P. G. *Chem. Phys. Lett.* **2003**, *371*, 349.
(34) Chaudhuri, D.; Balasubramanian, K. *Chem. Phys. Lett.* **2004**, *399*, 67.
(35) Parr, R. G.; Yang, W. *Density Functional Theory of Atoms and Molecules*; Oxford: New York, 1989.
(36) Møller, C.; Plesset, M. *Phys. Rev.* **1943**, *46*, 618.
(37) Becke, A. D. *J. Chem. Phys.* **1993**, *98*, 5648.
(38) Vosko, S. H.; Wilk, L.; Nusair, M. *Can. J. Phys.* **1980**, *58*, 1200.
(39) Lee, C. T.; Yang, W. T.; Parr, R. G. *Phys. Rev. B*: *Condens. Matter Mater. Phys.* **1988**, *37*, 785.
(40) Cances, E.; Mennucci, B.; Tomasi, J. *J. Chem. Phys.* **1997**, *107*, 3032.
(41) Mennucci, B.; Cances, E.; Tomasi, J. *J. Phys. Chem. B* **1997**, *101*, 10506.
(42) Mennucci, B.; Tomasi, J. *J. Chem. Phys.* **1997**, *106*, 5151.
(43) Tomasi, J.; Mennucci, B.; Cances, E. *J. Mol. Struct.: THEOCHEM* **1999**, *464*, 211.
(44) Hehere, W. J.; Radom, L.; Schleyer, P. V. R.; Pople, J. A. *Ab Initio Molecular Orbital Theory*; Wiley: New York, 1986.
(45) Ben-Naim, A. *J. Phys. Chem.* **1978**, *82*, 792.
(46) *NIST Chemistry WebBook*; U.S. National Institute of Standards and Techology: Gaithersburg, MD. http://webbook.nist.gov/chemistry
(47) Frisch, M. J.; Trucks, G. W.; Schlegel, H. B.; Scuseria, G. E.; Robb, M. A.; Cheeseman, J. R.; Zakrzewski, V. G.; Montgomery, J. A., Jr.; Stratmann, R. E.; Burant, J. C.; Dapprich, S.; Millam, J. M.; Daniels, A. D.; Kudin, K. N.; Strain, M. C.; Farkas, O.; Tomasi, J.; Barone, V.; Cossi, M.; Cammi, R.; Mennucci, B.; Pomelli, C.; Adamo, C.; Clifford, S.; Ochterski, J.; Petersson, G. A.; Ayala, P. Y.; Cui, Q.; Morokuma, K.; Salvador, P.; Dannenberg, J. J.; Malick, D. K.; Rabuck, A. D.; Raghavachari, K.; Foresman, J. B.; Cioslowski, J.; Ortiz, J. V.; Baboul, A. G.; Stefanov, B. B.; Liu, G.; Liashenko, A.; Piskorz, P.; Komaromi, I.; Gomperts, R.; Martin, R. L.; Fox, D. J.; Keith, T.; Al-Laham, M. A.; Peng, C. Y.; Nanayakkara, A.; Challacombe, M.; Gill, P. M. W.; Johnson, B.; Chen, W.; Wong, M. W.; Andres, J. L.; Gonzalez, C.; Head-Gordon, M.; Replogle, E. S.; Pople, J. A. *Gaussian 03*, revision C.02; Gaussian, Inc.: Pittsburgh, PA, 2005.

Table 1. Geometrical Parameters (Bond Distances in Å and Angles in deg) for Singlet and Triplet States (in Parentheses) of $NpO_2(CO_3)^-$ and $NpO_2(CO_3)(H_2O)_3^-$ and Their Energy Differences (in kcal/mol) at the DFT/B3LYP, MP2, and CCSD Levels

	$NpO_2(CO_3)^-$					$NpO_2(CO_3)(H_2O)_3^-$			
geometrical parameters	DFT (g)	MP2 (g)	CCSD (g)	DFT (aq)	MP2 (aq)	DFT (aq)	MP2 (aq)	Gagliardi and Roos (aq)[e]	exptl (aq)[f]
$r(Np-O_{ax})$[a]	1.819	1.860	1.815	1.802	1.827	1.796	1.830	1.836	1.84 ± 0.02
	(1.887)	(1.800)		(1.832)	(1.801)	(1.823)	(1.811)		
$r(Np-O)$[b]	2.274	2.242	2.256	2.429	2.402	2.463, 2.439	2.399, 2.412	2.475	2.49 ± 0.03
	(2.258)	(2.246)		(2.439)	(2.429)	(2.466, 2.451)	(2.417, 2.421)		
$r(Np-O_w)$[c]						2.623, 2.600, 2.628	2.540, 2.534, 2.554	2.570	
						(2.639, 2.616, 2.641)	(2.566, 2.567, 2.553)		
$r(Np-C)$	2.745	2.702	2.723	2.875	2.840	2.895	2.841	2.933	2.94 ± 0.03
	(2.735)	(2.709)		(2.886)	(2.869)	(2.905)	(2.858)		
$r(Np-O)$[d]	3.971	3.929	3.946	4.131	4.099	4.154	4.102	4.212	4.24 ± 0.03
	(3.956)	(3.939)		(4.143)	(4.132)	(4.165)	(4.121)		
$\theta(O_{ax}-Np-O_{ax})$	163.8	149.1	156.7	179.8	179.2	177.6	176.9		
	(152.3)	(164.2)		(179.6)	(179.1)	(176.6)	(176.5)		
$\Delta E_{singlet-triplet}$	26.45			24.45		28.29	19.68		

[a] The An=O axial bonds. [b] Neptunium connected to carbonate oxygens. [c] Neptunium to water's oxygen distance. [d] The O atom is the last O connected only to carbon farthest away from Np. [e] Reference 17. [f] Reference 13.

phase and in aqueous solution. We have also optimized the structures of $NpO_2(CO_3)^-$, $NpO_2(CO_3)_2^{3-}$, and $NpO_2(CO_3)_3^{5-}$ at both the CCSD and the MP2 levels in the gas phase to calibrate our results with the previous CASSCF/CASPT2 computations of these complexes. Once we had established that our MP2 techniques offer reliable results, we then proceeded to optimize $NpO_2(CO_3)_m(H_2O)_n^{q-}$ ($m = 1-3$, $n = 0-3$) in aqueous solution through the PCM continuum model at both the DFT/B3LYP and the MP2 levels. The equilibrium geometries are presented in Tables 1−5. The optimized structures at the MP2 level in solution are also shown in Figure 1.

Table 1 shows the computed structural parameters for the naked $NpO_2(CO_3)^-$ complex in the gas phase at three levels of theory together with the solution structures for the hydrated complex $NpO_2(CO_3)(H_2O)_3^-$. Figure 1 shows the computed equilibrium geometries of several structures, among which the naked monocarbonate is shown in part a of Figure 1. Interestingly, at all levels of theory, the O=Np=O axial bond is bent in the gas phase for the monocarbonate and is akin to the corresponding structure of $UO_2(CO_3)$ that we have studied earlier in the gas phase.[32] However, as can be seen from Table 1, the O=Np=O axial bond is almost linear for $NpO_2(CO_3)^-$ in solution as well as for the hydrated $NpO_2(CO_3)(H_2O)_3^-$ complex (Figure 1b) in aqueous solution. The bent axial bond for the naked complex in the gas phase is due to the single carbonate, which cannot bind to the orbitals on both sides. This artifact is removed once the complex is placed in aqueous solution or when the complex is stabilized through bound water molecules in the gas phase or if more carbonate ligands are added. We note from Table 1 that the three methods considered here (DFT, MP2, and CCSD) give reasonable descriptions, but the DFT method gives somewhat larger values for nonbonded distances and does not perform very well for water molecules bonded to Np, and for this reason we have not considered using the DFT method for other larger water-bound complexes in solution. For the singlet states of these complexes, the DFT method tends to yield shorter O=Np=O bond distances uniformly even after three water molecules are added to the complex. This discrepancy

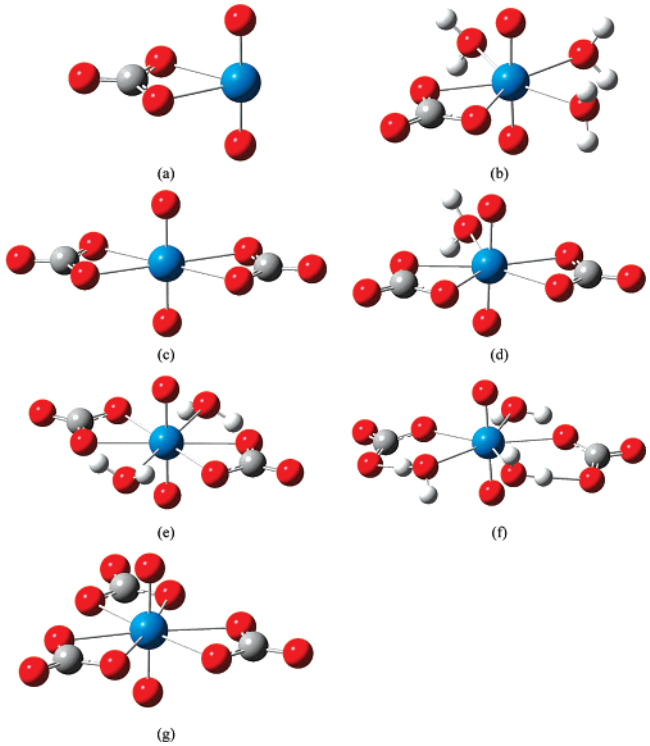

Figure 1. The optimized (a) $NpO_2(CO_3)^-$, (b) $NpO_2(CO_3)(H_2O)_3^-$, (c) $NpO_2(CO_3)_2^{3-}$, (d) $NpO_2(CO_3)_2(H_2O)^{3-}$, (e) $NpO_2(CO_3)_2(H_2O)_2^{3-}$, (f) $NpO_2(CO_3)_2(H_2O)_3^{3-}$, and (g) $NpO_2(CO_3)_3^{5-}$ complexes in aqueous solution.

of almost 0.04 Å at the DFT level (Table 1) in aqueous solution for the O=Np=O distances in $NpO_2(CO_3)(H_2O)_3^-$ is definitely due to the inadequate DFT description of the equatorial $Np-OH_2$ interactions. It can be seen from Table 1 that the addition of water molecules quantum chemically bound to the complex elongate the O=Np=O axial bond, as expected due to the competition of water molecules in bonding to Np. However, in the case of open-shell states, the Np=O bond is longer at the DFT/B3LYP level than that at the MP2 level due to significant electron correlation effects arising from open-shell orbitals. For $NpO_2(CO_3)^-$, the Np=O bond distance is 1.887 and 1.832 Å at the DFT/B3LYP level in the gas phase and in aqueous solution, respectively,

Table 2. Geometrical Parameters (Bond Distances in Å and Angles in deg) for Singlet and Triplet States (in Parentheses) of $NpO_2(CO_3)_2^{3-}$ and Their Energy Differences (in kcal/mol) at the DFT/B3LYP, MP2, and CCSD Levels

geometrical parameters	DFT (g)			MP2 (g)	CCSD (g)	DFT (aq)	MP2 (aq)	Gagliardi and Roos (aq)[f]
	78 *e* RECP	68 *e* RECP[d]	60 *e* RECP[e]					
$r(Np-O_{ax})$[a]	1.816	1.901	1.861	1.847	1.856	1.817	1.830	1.850
	(1.825)	(1.931)	(1.879)	(1.804)		(1.825)	(1.804)	
$r(Np-O)$[b]	2.489	2.484	2.452	2.444	2.443	2.471, 2.481, 2.473, 2.484	2.461, 2.462, 2.462, 2.461	2.548
	(2.508)	(2.485)	(2.462)	(2.482)		(2.504, 2.508, 2.506, 2.510)	(2.485, 2.487, 2.486, 2.488)	
$r(Np-C)$	2.932	2.922	2.893	2.877	2.888	2.919	2.896	2.970
	(2.955)	(2.927)	(2.905)	(2.920)		(2.954)	(2.925)	
$r(Np-O)$[c]	4.199	4.185	4.154	4.148	4.151	4.179	4.162	4.290
	(4.223)	(4.189)	(4.167)	(4.193)		(4.222)	(4.198)	
$\theta(O_{ax}-Np-O_{ax})$	180.0	180.0	180.0	180.0	180.0	180.0	180.0	
	(180.0)	(180.0)	(180.0)	(180.0)		(180.0)	(180.0)	
$\Delta E_{singlet-triplet}$	33.64	24.04	26.60	17.94			20.64	

[a] The An=O axial bonds. [b] Neptunium connected to carbonate oxygens. [c] The O atom is the last O connected only to the carbon farthest away from Np. [d] The Stuttgart basis set and the 60-electron RECP for Np. 6-311G(p) for C and O. [e] Christiansen's unpublished basis set and the 68-electron RECP for Np. 6-311G(p) for C and O. [f] Reference 17. CASSCF/CASPT2 using a reaction field Hamiltonian in a spherical cavity.

while it is 1.800 and 1.801 Å, respectively, at the MP2 level. Moreover, it is to be noted that the triplet state is lower than the singlet state.

The Np(V) oxidation state yields the $NpO_2(CO_3)_2^{3-}$ ion that has a D_{2h} equilibrium structure with the neptunyl axial part (O=Np=O) perpendicular to the rest of the molecular system (Figure 1c and Table 2). The MP2 and the DFT/B3LYP levels of theory yield comparable results with the exception that the DFT method yields artificially shorter O=Np=O axial bonds for the singlet states at the cost of elongated Np−O and Np−C equatorial distances, which are influenced by dispersion interactions. However, for the triplet states of these complexes, the DFT method yields longer O=Np=O axial bond lengths than those of the MP2 method due to the significant electron correlation effects of open-shell orbitals, whereas the Np−O and Np−C equatorial distances are still elongated at the DFT/B3LYP level. As can be seen from Table 2, the MP2 results agree quite well with those of the CCSD method in the gas phase and this agreement provides confidence in the MP2 results. Moreover, the CCSD method for geometry optimization and frequency computations is computationally very intensive, and consequently, the MP2 method is a more viable alternative for these complexes. It is not currently feasible to do the CCSD computations in solution. It is also important to recognize that the Np−C bond distances differ significantly; that is, as can be seen from Table 2, the Np−C distances are 2.932 and 2.877 Å at the DFT/B3LYP and MP2 levels, respectively. This is not surprising in view of the fact that the MP2 method accounts for the various interactions properly, and such interactions are especially important for nonbonded Np−C interactions. Moreover, it is to be noted that the Stuttgart basis set and the 60-electron RECP for Np performed very well. The DFT results obtained using the Stuttgart 60-electron RECPs are consistent with the CCSD results obtained employing 78-electron large core potentials and the corresponding basis set. However, the optimization and frequency computations with the Stuttgart basis set are quite intensive computationally even at the DFT level.

The results presented in Table 2 show that the neptunium−oxygen axial distances shorten by 0.017 Å after $NpO_2(CO_3)_2^{3-}$ is embedded in solution at the MP2 level, whereas the corresponding DFT distances increase by 0.001 Å. Furthermore, the Np−O equatorial bond distances elongate by 0.022 Å at the MP2 level, while the DFT method yields aqueous-phase Np−O equatorial distances that are up to 0.018 Å shorter. The decrease in the equatorial bond distances is not offset by a corresponding increase in the O=Np=O axial distances at the DFT level. This is more evidence that the long-range solvent effects, which seem to be important for the geometries in solution, are not adequately treated by the DFT method.

The trihydrated neptunyl monocarbonate and monohydrated and dihydrated neptunyl dicarbonate complexes, i.e., $NpO_2(CO_3)(H_2O)_3^-$ (Figure 1b), $NpO_2(CO_3)_2(H_2O)^{3-}$ (Figure 1d), and $NpO_2(CO_3)_2(H_2O)_2^{3-}$ (Figure 1e), were optimized in aqueous solution through the PCM continuum model at the DFT/B3LYP and MP2 levels. It is essential that water molecules be included in the chemical bonding to the complex for a realistic treatment of the complex in aqueous solution, as the naked complex without H_2O molecules does not represent the actual first hydration sphere of the aqueous complex. Our computations reveal that the water molecules in the optimized geometries lie in the equatorial plane that contains neptunium and carbonates. As can be seen from Figure 1e, the dicarbonate complex has a hexacoordinated equatorial structure with two water molecules bound to neptunium equatorially in the first coordination shell. In order to juxtapose the structures in aqueous solution and in the gas phase, we have also optimized the supermolecules in the gas phase. We found a dramatic difference between the optimized structures in the gas phase and aqueous solution for the hydrated complex of dicarbonate. In the gas phase, the lowest energy structure exhibits water molecules that are bound to the carbonate part instead of directly to neptunium as in the $NpO_2(CO_3)_2(H_2O)^{3-}$ and $NpO_2(CO_3)_2(H_2O)_2^{3-}$ clusters both optimized at the DFT/B3LYP and MP2 levels.

Clark et al.[13] have experimentally determined the geometries of some related neptunium carbonate complexes using EXAFS spectroscopy. For $NpO_2(CO_3)_2^{3-}$, the Np−O axial bond and equatorial distances are 1.85 and 2.48 Å in solution, respectively. The Np−C distances were found to be 2.93 Å. Our MP2 axial Np−O, equatorial Np−O, and Np−C distances are 1.843, 2.494, 2.498, 2.935, and 2.937 Å for

Table 3. Geometrical Parameters (Bond Distances in Å and Angles in deg) for Singlet and Triplet States (in Parentheses) of $NpO_2(CO_3)_2(H_2O)^{3-}$ and $NpO_2(CO_3)_2(H_2O)_2^{3-}$ and Their Energy Differences (in kcal/mol) in Aqueous Solution at the DFT/B3LYP and MP2 Levels

	$NpO_2(CO_3)_2(H_2O)^{3-}$		$NpO_2(CO_3)_2(H_2O)_2^{3-}$			
geometrical parameters	DFT	MP2	DFT	MP2	Gagliardi and Roos[e]	exptl[f]
$r(Np-O_{ax})$[a]	1.815 (1.826)	1.839 (1.816)	1.765 (1.829)	1.843 (1.817)	1.854	1.85 ± 0.02
$r(Np-O)$[b]	2.536, 2.526, 2.447, 2.447 (2.499, 2.493, 2.489, 2.486)	2.490, 2.480, 2.432, 2.429 (2.467, 2.460, 2.451, 2.444)	2.564, 2.557, 2.566, 2.559 (2.535, 2.532, 2.537, 2.536)	2.498, 2.494, 2.498, 2.496 (2.501, 2.498, 2.502, 2.501)	2.548	2.48 ± 0.03
$r(Np-O_w)$[c]	2.636 (2.617)	2.555 (2.549)	2.701, 2.698 (2.688, 2.679)	2.624, 2.618 (2.608, 2.603)	2.585	
$r(Np-C)$	2.930, 2.925 (2.932, 2.931)	2.892, 2.887 (2.887, 2.886)	2.999, 2.998 (2.980, 2.979)	2.937, 2.935 (2.942, 2.940)	2.891	2.93 ± 0.03
$r(Np-O)$[d]	4.193, 4.188 (4.196, 4.194)	4.159, 4.155 (4.155, 4.154)	4.249 (4.247, 4.246)	4.209, 4.207 (4.214, 4.212)	4.244	4.18 ± 0.03
$\theta(O_{ax}-Np-O_{ax})$	178.3 (177.8)	177.8 (177.8)	180.0 (180.0)	180.0 (179.9)		
$\Delta E_{singlet-triplet}$	31.13	19.96		19.54		

[a] The An═O axial bonds. [b] Neptunium connected to carbonate oxygens. [c] Neptunium to water's oxygen distance. [d] The O atom is the last O connected only to the carbon farthest away from Np. [e] Reference 17; CASSCF/CASPT2 using a reaction field Hamiltonian in a spherical cavity. [f] Reference 13.

the singlet state and 1.817, 2.498, 2.502, 2.940, and 2.942 Å for the triplet states, respectively, in good agreement with Clark et al.'s experimental results.[13] This provides further confidence in the MP2 computations in aqueous solution and that the DFT method yields O═Np═O axial bond lengths that are too short.

It should be noted that there is a uniform increase of the axial Np−O bond lengths when the number of water molecules increases in the fist hydration sphere, and they are all longer than the corresponding gas-phase Np═O distances. The Np═O axial bond length is 1.843 Å in $NpO_2(CO_3)_2(H_2O)_2^{3-}$, compared with 1.839 Å in $NpO_2(CO_3)_2(H_2O)^{3-}$. The equatorial Np−O distances (Np atom connected with the carbonate oxygen) also increase from mono- to dihydrated complexes. The results show that the influence of the solvent is observable in the optimized geometries of these continuum calculations.

Clark et al.[13] are uncertain about the number of water molecules bound to $NpO_2(CO_3)_2^{3-}$. Thus, we have also optimized the structure of $NpO_2(CO_3)_2(H_2O)_3^{3-}$ in solution. As can be seen from Figure 1f, in $NpO_2(CO_3)_2(H_2O)_3^{3-}$, neptunyl is five-coordinated. Three water molecules are bound to neptunium in the equatorial plane with O═Np═O in the axial position. However, the other two water molecules insert between carbonate ligands and neptunium to form five-membered rings. Thus, we conclude that two water molecules directly bind to $NpO_2(CO_3)_2^{3-}$ in the first solvation shell.

Gagliardi and Roos[17] have carried out high-level CASSCF/CASPT2 computations of the naked and hydrated complex by modeling the solvent effect by a reaction field Hamiltonian with a spherical cavity. Considering that the MP2 level is based on a single-reference method, it is at a lower level compared with the CASPT2 method. However, as can be seen from Tables 1−3, our computed results in the liquid phase at the MP2 level are in very good agreement with the CASPT2 results, presumably due to the predominant single-reference character of the ground states of these complexes. Our computed geometrical parameters also support the conclusion of Gagliardi and Roos[17] that the monocarbonate

Table 4. Geometrical Parameters (Bond Distances in Å and Angles in deg) for Singlet and Triplet States (in Parentheses) of $NpO_2(CO_3)_2(H_2O)_3^{3-}$ and Their Energy Differences (in kcal/mol) in Aqueous Solution at the DFT/B3LYP and MP2 Levels

geometrical parameters	DFT	MP2
$r(Np-O_{ax})$[a]	1.798. 1.800 (1.817, 1.821)	1.825, 1.828
$r(Np-O)$[b]	2.395, 2.547 (2.427, 2.541)	2.367, 2.493
$r(Np-O_w)$[c]	2.688, 2.581, 2.597 (2.708, 2.578, 2.583)	2.611, 2.537, 2.555
$\theta(O_{ax}-Np-O_{ax})$	179.2 (179.4)	179.1
$\Delta E_{singlet-triplet}$	25.71	

[a] The An═O axial bonds. [b] Neptunium connected to carbonate oxygens. [c] Neptunium to water's oxygen distance.

has a pentacoordinated structure with three H_2O molecules bound to it in aqueous solution whereas the dicarbonate structure carries two water molecules and is hexacoordinated. As can be seen from Table 5, only in the case of tricarbonate $NpO_2(CO_3)_3^{5-}$ do our computed structural parameters differ from those of Gagliardi and Roos,[17] primarily because their computations were carried out in the gas phase using counterions. As can be seen from Table 5, the counterions do not accurately model the solvation effects as the counterions tend to elongate the neptunyl axial bonds as well as the Np−O equatorial bonds. Moreover, although $NpO_2(CO_3)_3^{5-}$ has D_{3h} symmetry in the gas phase, it is less likely to retain the same symmetry in aqueous solution because of the solvent interactions. We have also reported the IR spectra and vibrational frequencies of these species both in the gas phase and in aqueous solution, which have not been computed previously.[17]It is also interesting that our numerically most intensive CCSD computations validated the MP2 method in the gas phase reasonably well, but the computations of CCSD vibrational frequencies were very intensive, requiring over a month of CPU time on an Itanium cluster. This, combined with the validation of our solution-phase computations with the CASSCF/CASPT2 method of Gagliardi and Roos[17] shows that the MP2 method is a reliable and

Table 5. Geometrical Parameters (Bond Distances in Å and Angles in deg) for Singlet and Triplet States (in Parentheses) of $NpO_2(CO_3)_3^{5-}$ and Their Energy Differences (in kcal/mol) at the DFT/B3LYP and MP2 Levels

geometrical parameters	DFT (aq)	MP2 (aq)	Gagliardi and Roos (g)[d]	exptl[e]
$r(Np-O_{ax})$[a]	1.829 (1.846)	1.867, 1.858 (1.828)	1.876	1.86 ± 0.02
$r(Np-O)$[b]	2.548−2.619, (2.581−2.589)	2.503−2.545 (2.528−2.540)	2.598	2.53 ± 0.03
$r(Np-C)$	3.026, 3.027, 3.054 (3.035, 3.030, 3.030)	2.961, 2.965, 2.982 (2.974, 2.975, 2.977)	2.974	2.98 ± 0.03
$r(Np-O)$[c]	4.300, 4.301, 4.331 (4.310, 4.305, 4.306)	4.239, 4.244, 4.262 (4.254, 4.255, 4.257)	4.361	4.22 ± 0.03
$\theta(O_{ax}-Np-O_{ax})$	179.9 (179.9)	179.7 (179.9)		
$\Delta E_{singlet-triplet}$	34.59	21.23		

[a] The An═O axial bonds. [b] Neptunium connected to carbonate oxygens. [c] The O atom is the last O connected only to the carbon farthest away from Np. [d] Reference 17; CAS/CASPT2 in the gas phase using counterions. [e] Reference 13.

Table 6. Calculated Vibrational Harmonic Frequencies ν_{ss} and ν_{as} (cm^{-1}) in Aqueous Solution at the Different Levels of Theory (IR Intensities Given in Parentheses)

	B3LYP		MP2		exptl	
	ss	as	ss	as	ss	as
NpO_2^+	792(0.0849)	860(886.0349)	793(0.0778)	856(846.4132)	767[a]	824[b]
$NpO_2(CO_3)^-$	745(0.0682)	782(1054.0274)	760(1.1664)	789(975.4779)	762[c]	
$NpO_2(CO_3)(H_2O)_3^-$	757(21.8528)	770(1130.5377)	751(0.3704)	763(1093.5846)		
$NpO_2(CO_3)_2^{3-}$	667(0.0432)	710(1274.0206)	699(0.2535)	747(1170.6424)	756[c]	
$NpO_2(CO_3)_2(H_2O)^{3-}$	637(14.5033)	662(1338.0209)	693(16.6209)	724(1267.9910)		
$NpO_2(CO_3)_2(H_2O)_2^{3-}$	777(1.3321)	786(1621.7602)	683(1.2512)	706(616.8128)		
$NpO_2(CO_3)_2(H_2O)_3^{3-}$	726(115.1270)	747(1066.6419)	731(228.8145)	762(882.6204)		
$NpO_2(CO_3)_3^{5-}$	629(1.1601)	648(1492.7614)			756[c]	

[a] Reference 49. [b] Reference 50. [c] Reference 12.

pragmatic method of choice for the study of these complexes in solution, provided that the complexes are predominantly single-reference in nature.

Clark and co-workers[12] have employed an innovative technique to enhance the solubility of neptunyl carbonate ions by using the solubility-enhancing tetrabutylammonium cation instead of the commonly used Na^+ and K^+ solutions containing pure samples of the well-characterized molecular species $NpO_2(CO_3)^-$, $NpO_2(CO_3)_2^{3-}$, and $NpO_2(CO_3)_3^{5-}$. Once the solubilities of these species were enhanced, the Raman spectra of these species could be measured. The Raman frequencies for the symmetric O═Np═O stretch of $NpO_2(CO_3)^-$, $NpO_2(CO_3)_2^{3-}$, and $NpO_2(CO_3)_3^{5-}$ were observed at 762, 756, and 756 cm^{-1}, respectively. They have reassigned the 755 cm^{-1} peak[48] reported previously for an unstable neptunyl(V) solution in 2 M carbonate as indeed being due to the solution species $NpO_2(CO_3)_3^{5-}$.

We have obtained the vibrational spectra and all the vibrational frequencies of the monocarbonate complex at the CCSD, MP2, and DFT levels, while the computed spectra and frequencies of the larger complexes were obtained using the MP2 and DFT methods. Among our computed frequencies, the O═Np═O axial stretching harmonic vibrational frequencies of the carbonates are of particular interest. Solvent effects on the spectra were also studied at the DFT/B3LYP and MP2 levels using the self-consistent reaction field PCM models. The resulting values of the vibrational frequencies in solution are shown in Table 6 along with neptunyl(V) frequencies, which illustrate the effect of carbonate complexation as well as solvation on the strength of the actinyl bond. The complete IR spectra are also presented in Figure 2. For the $NpO_2(CO_3)_2(H_2O)_2^{3-}$ cluster, the O═Np═O stretching frequencies are obtained at 777 (symmetric) and 786 cm^{-1} (antisymmetric) using the DFT/B3LYP method. The corresponding values are 683 (symmetric) and 706 cm^{-1} (antisymmetric) at the MP2 level. The DFT/B3LYP results tend to be higher, which is consistent with the shorter O═Np═O bonds obtained at the B3LYP level. It is to be noted that there is a strong CO_2-scissor vibration at 720 cm^{-1}, which couples with the symmetric O═Np═O stretching vibration. As a consequence, the ν_{ss} symmetry stretch frequency is split as 683 and 737 cm^{-1} at the MP2 level.

As can be seen from Table 6, the calculated O═Np═O symmetric stretching frequency decreases from NpO_2^+ (793 cm^{-1}, MP2) to $NpO_2(CO_3)_2^{3-}$ (699 cm^{-1}, MP2). This is consistent with the decreasing O═Np═O bond strength due to equatorial bonding with the carbonate ligand. The trend is also observed in the antisymmetric stretching frequencies. This shows that the neptunyl ν_{ss} and ν_{as} stretch frequencies undergo measurable red-shifts upon carbonate complexation. Carbonate ligands transfer electron density to the neptunyl ion, which in turn destabilizes the 6d orbitals and thereby weakens the neptunyl O═Np═O bonds. Moreover, due to the elongation of the O═Np bonds upon solvation as a

(48) Madic, C.; Hobart, D. E.; Begun, G. M. *Inorg. Chem.* **1983**, *22*, 1494.
(49) Tait, C. D. In *Book of Abstracts, Symposium on Heavy Element Complexes: The Convergence of Theory and Experiment*; 217th ACS National Meeting, Anaheim, CA, March 21−25, 1999; American Chemical Society: Washington, DC, 1999.
(50) Jones, L. H.; Penneman, R. A. *J. Chem. Phys.* **1953**, *21*, 542.

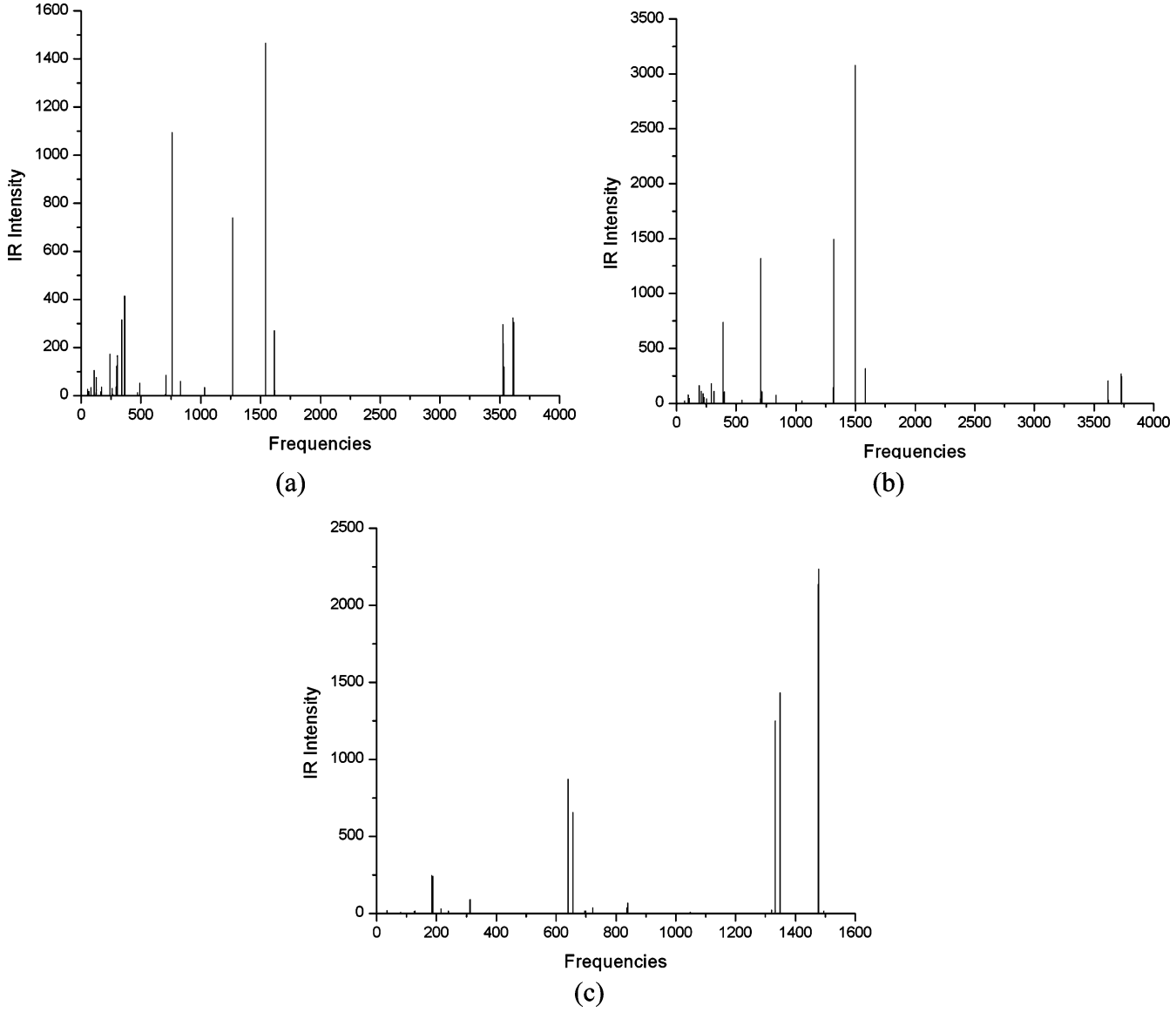

Figure 2. Computed IR spectra of singlet states of (a) $NpO_2(CO_3)(H_2O)_3^-$, (b) $NpO_2(CO_3)_2(H_2O)_2^{3-}$, and (c) $NpO_2(CO_3)_3^{5-}$ in aqueous solution.

Table 7. Calculated Mulliken Population Charges (Electrons) for Singlet and Triplet States (in Parentheses) of $NpO_2(CO_3)_2(H_2O)_n^{3-}$ ($n = 0-3$) in Aqueous Solution and the Gas Phase

	gross population of Np								
	s	p	d	f	q(Np)	q(O_{ax})	q(NpO_2^+)	q(CO_3^{2-})	q(H_2O)
NpO_2^+(aq)	1.95	6.07	0.85	3.61	2.52	−0.76	1.00		
	(1.95)	(6.07)	(0.87)	(3.64)	(2.48)	(−0.74)	(1.00)		
$NpO_2(CO_3)_2^{3-}$(aq)	1.91	6.09	1.21	3.69	2.01	−0.86	0.29	−1.64	
	(1.93)	(6.14)	(1.33)	(3.76)	(1.85)	(−0.79)	(0.27)	(−1.64)	
$NpO_2(CO_3)_2^{3-}$(g)	1.92	6.14	1.32	3.73	1.79	−0.82	0.16	−1.58	
	(1.92)	(6.14)	(1.33)	(3.76)	(1.85)	(−0.79)	(0.27)	(−1.64)	
$NpO_2(CO_3)_2(H_2O)^{3-}$(aq)	1.93	6.07	1.29	3.67	2.02	−0.90	0.22	−1.65	0.08
$NpO_2(CO_3)_2(H_2O)_2^{3-}$(aq)	1.90	6.09	1.27	3.65	2.08	−0.95	0.18	−1.67	0.08
	(1.89)	(6.09)	(1.28)	(3.66)	(2.08)	(−0.89)	(0.30)	(−1.72)	(0.07)
$NpO_2(CO_3)_2(H_2O)_3^{3-}$(aq)	1.95	6.07	1.30	3.68	1.97	−0.84, −0.89	0.25	−1.68, −1.70	0.03, 0.04, 0.06

consequence of the dielectric cavity, the O═Np═O axial stretching frequencies exhibit red-shifts with respect to free $NpO_2(CO_3)_2^{3-}$. When the clusters have explicitly bound H_2O molecules in the first hydration sphere, that is, quantum chemically bound H_2O molecules in the continuum model, the solvent-induced frequency changes are even more conspicuous, as can be seen from Table 6.

The analysis of the bonding characteristics of $NpO_2(CO_3)_2^{3-}$ can be made through the consideration of the Mulliken populations. Table 7 shows the gross population of Np, the total Mulliken charge for Np and axial O atoms, as well as the charges on the various fragments in the hydrated neptunyl bicarbonate complexes. For $NpO_2(CO_3)_2^{3-}$, the MP2 calculation shows that the neptunyl portion has an overall charge

Table 8. Solvation Gibbs Energies, ΔG^* (kcal/mol) of Singlet States of $NpO_2(CO_3)_2^{3-}$ at the MP2 and DFT/B3LYP (in Parentheses) Levels

	$n\Delta G_{vap}(H_2O)$	ΔG^*_{clust}	$\Delta G^*_{solv}(S(H_2O)_n)$	$\Delta G^*_{solv}(S)$
$NpO_2(CO_3)_2^{3-}$				−394.22 (−384.54)
$NpO_2(CO_3)_2(H_2O)^{3-}$	1.48	15.13 (19.65)	−413.46 (−407.00)	−396.85 (−385.87)
$NpO_2(CO_3)_2(H_2O)_2^{3-}$	2.96	65.87 (23.56)	−404.62 (−400.55)	−335.79 (−374.03)

of 0.16 for the singlet state and 0.27 for the triplet state, while the carbonate has an overall charge of −1.58 for the singlet state and −1.64 for the triplet state, indicating that there is a charge transfer of 0.42 for the singlet state and 0.36 for the triplet state from each carbonate ligand to neptunyl. It is also interesting that the charge of 2.52 on Np in free NpO_2^+ is reduced to 2.01 in the aqueous dicarbonate complex, suggesting a transfer of 0.51 from the carbonate ligand to singlet NpO_2^+. As can be seen in Table 7, the carbonate ligands transfer electron density mostly to the Np-(6d) orbital, 0.47 *e* in the gas phase and 0.36 *e* in aqueous solution, respectively.

The calculated gross Mulliken population charges, for gas-phase $NpO_2(CO_3)_2^{3-}$, on Np and the axial oxygens at the MP2 level are 1.79 and −0.82 for the singlet state, respectively. The corresponding values for the triplet state differ slightly as 1.85 and −0.79 for the respective atoms. In both cases, this is indicative of charge delocalization between the Np and O atoms, and thus the π character of neptunyl bonding is not altered significantly, although it is weakened in $NpO_2(CO_3)_2^{3-}$. These data show that the neptunium 7s, 6d, and 5f orbitals have reduced populations compared with the $7s^25f^46d^1$ configuration of the dissociated Np atom, whereas the axial oxygens are electron rich in the 2p orbitals and deficient in the 2s orbitals. Thus, there is a strong overlap between the oxygen 2p and 2s orbitals with the neptunium 7s, 6d, and 5f orbitals. Upon addition of the carbonate ligands to NpO_2^+, Np positive charge is decreased and the O_{ax} electronic charge is increased, thus diminishing the covalent overlap between neptunium and the axial oxygen atoms inducing the elongation of the Np−O axial bond distances.

Next, we consider the spin−orbit effects of the $[NpO_2^+(CO_3)_m]^{q-}$ complexes. On the basis of the Mulliken population analysis of the electronic states both in the gas phase and in solution, the spin−orbit effects on the $[NpO_2^+(CO_3)]^{q-}$ complex can be estimated by considering the corresponding states of NpO_2^+. As discussed before, we have to consider the singlet and triplet states, and we expect the singlet electronic states to be little affected by spin−orbit coupling. The spin−orbit splitting is expected to be larger only for the triplet state, among the low-lying states, and we have estimated this by a comparison to the corresponding results for the uncomplexed NpO_2^+ in the gas phase obtained by Pitzer and coworkers.[51] We have arrived at this estimate by a weighted averaging of the computed gas-phase $^3H(6_g)-{}^3H(4_g)$ and $^3H(6_g)-{}^3H(5_g)$ splittings of the free NpO_2^+ (8867 and 4721 cm^{-1}, respectively) and by scaling the result with the respective 5f Mulliken populations of the triplet state of the free NpO_2^+ and the complexes that we have computed. We have thus obtained an upper bound for the spin−orbit stabilization of the triplet state of all the carbonate complexes considered here as 4200 cm^{-1}. The bond lengths and equilibrium geometries of the complexes that we have computed here are not expected to be impacted by the spin−orbit effects because the open-shell 5f orbitals of Np in these complexes do not take part in the bonding with ligands to an appreciable extent. Thus, we conclude that although the spin−orbit effects are negligible for the geometries, the energy separations of the open-shell electronic states are influenced by spin−orbit coupling.

The solvent effect is conspicuous in the charge distribution in that the net charge on NpO_2^+ changes from 0.16 in the gas phase to 0.29 for the singlet state in the solvent. This is countered by an increase in the negative charge by 0.06 *e*/carbonate. Interestingly, the explicit addition of water molecules has a minuscule effect on the charge distribution as evidenced from the Mulliken populations shown in Table 7. In the case of $NpO_2(CO_3)_2(H_2O)^{3-}$ and $NpO_2(CO_3)_2(H_2O)_2^{3-}$, the charges transferred from the carbonate ion to neptunyl are 0.78 and 0.82 *e*, respectively, compared with 0.71 *e* in $NpO_2(CO_3)_2^{3-}$.

The solvation Gibbs energy of $NpO_2(CO_3)_2^{3-}$ has been obtained from the thermodynamic cycle presented in Scheme 1. The relevant data and the calculated solvation Gibbs energies are summarized in Table 8. Although the continuum contribution ($\Delta G^*_{solv}(S(H_2O)_n)$) is larger than the discrete contribution ($\Delta G_{vap} + \Delta G^*_{clust}$), the direct solute−solvent interactions are still important, and thus, they should be included explicitly. As can be seen from Table 8, the solvation Gibbs energies of $NpO_2(CO_3)_2^{3-}$ are −385.87 kcal/mol (monohydrated) and −374.03 kcal/mol (dihydrated) at the DFT/B3LYP level. In the case of MP2 calculations, the corresponding values are −396.85 and −335.79 kcal/mol. The DFT/B3LYP and MP2 methods in conjunction with the discrete−continuum model for the solvation Gibbs energies differ by 40 kcal/mol, although they are very similar in the continuum model, as mentioned below. The difference is mainly due to the cluster Gibbs energies ΔG^*_{clust} in the gas phase. As shown in our previous paper,[25] the MP2 result is close to the most accurate CCSD result for bond energies when a single-reference configuration dominates. Thus, we believe that the MP2 results presented here are more reliable for the solvation Gibbs energies in the discrete−continuum model.

We have also employed a pure continuum IEFPCM model and united atom radii without quantum chemically bound H_2O molecules by using the DFT/B3LYP and MP2 methods to compute the solvation Gibbs energy of $NpO_2(CO_3)_2^{3-}$. The values thus obtained are −384.54 and −394.22 kcal/mol at the DFT/B3LYP level and MP2 levels, respectively. Evidently, a pure continuum model is ineffective in obtaining

(51) Matsika, S.; Pitzer, R. M. *J. Phys. Chem. A* **2000**, *104*, 4064.

the solvation energies of naked charged species in aqueous solution, as completing the first hydration sphere quantum mechanically is essential to an accurate description of the solvated species. This is a consequence of the fact that it is difficult to define the cavity radius for the unhydrated charged species. The mixed discrete−continuum model, where the first solvation shell is explicitly included in the solute definition, seems to be a more definitive way to study the solvation of charged species. As we show here, the explicit inclusion of the first solvent shell makes this model less dependent on the cavity size selection.

4. Conclusions

In the work, we have presented the optimized structures of a variety of hydrated neptunyl carbonate complexes, i.e., $NpO_2(CO_3)_m(H_2O)_n^{q-}$ ($m = 1-3$, $n = 0-3$), in aqueous solution. For the first time, we have computed their IR spectra and vibrational frequencies both in the gas phase and aqueous solution and reported the nature of bonding in these species. The structural and vibrational results in aqueous solution at the MP2 level are in good agreement with Clark et al.'s experiments and provide realistic pictures of these complexes in aqueous solution. It is interesting to note that we have found considerable mixing of neptunyl stretching with CO_2-scissor vibrations. Moreover, solvation Gibbs energies of free $NpO_2(CO_3)_2^{3-}$ have been calculated as −394.22 kcal/mol at the MP2 level. This value differs from the corresponding values of −396.85 (monohydrated) and −335.79 kcal/mol (dihydrated) obtained by using a discrete−continuum model at the MP2 level. Thus the first solvation shell was treated quantum chemically before considering a continuum model due to the indeterminate nature of the dielectric cavity radii. Moreover, the DFT method is not robust for computing the properties of solvated species, as this method yields solvation energies that differ by as much as 40 kcal/mol and substantial structural and spectral differences for solvated species. Our computed IR spectra and the predicted red-shifts due to solvation effects are in accord with experiment. We have compared the gas-phase results obtained at the MP2 level with more accurate and intensive CCSD methods and have shown that the MP2 method has the efficacy and efficiency to treat the molecules both in the gas phase and in an aqueous environment. Our computed MP2 results in aqueous solution for the mono- and dicarbonates also agree with the CASSCF/CASPT2 reaction field with a spherical solvent cavity methods of Gagliardi and Roos,[17] thus confirming the predominantly single-reference nature of these species. However, we found noticeable differences in the tricarbonate complexes treated in solution compared with those in the previous gas-phase study.[17]

Acknowledgment. This research was supported by the U.S. Department of Energy under Grant No. DEFG2-05ER15657. The work at Lawrence Livermore National Laboratory was performed under the auspices of the U.S. Department of Energy by the University of California under Contract No. W-7405-Eng-48.

IC700486U